euspen's 26th International Conference & Exhibition, Krakow, PL, June 2026
www.euspen.eu

Probe head errors module for digital-metrological twin of five-axis CMM based on use of neural networks

Piotr Gąska[1], Wiktor Harmatys[2], Maciej Gruza[2], Adam Gąska[2]

[1]*AGH University of Krakow, Faculty of Mechanical Engineering and Robotics*
[2]*Cracow University of Technology, Faculty of Mechanical Engineering*

adam.gaska@pk.edu.pl

Abstract
Currently, in the era of Industry 4.0, smart factories, and digital manufacturing also in the field of metrological solutions, which form the basis of quality control systems in production, many new concepts are emerging that aim to minimize human intervention in the measurement process, its evaluation, and the assessment of measurement accuracy. Example of such solutions are digital-metrological twins, which are used to synchronize the digital representation of a measurement system or process with the actual state of real system or process. Digital metrological twins of coordinate measuring systems typically consist of several modules that replicate and simulate the errors of individual CMM subsystems (e.g., a module simulating kinematic errors of the CMM or errors of the measuring probe) or factors that affect the accuracy of measurements performed on a CMM (e.g., a module simulating the influence of temperature or vibrations). This article presents the concept of a new module that simulates probe head errors, based on the application of neural networks, for use in a digital metrological twin of a five-axis CMM. The article presents experiments based on measuring standard rings in different orientations, that aim at determining error distributions of probe heads used in five-axis CMMs. A method is also presented for simulating measurement errors in arbitrary probe head orientations, using data obtained in the aforementioned phase together with neural networks. The correctness of the developed module is verified by comparing its results with experimentally obtained error values, for points different from those used in the process of identification of the probe head error distributions. The verification results proved that the errors simulated by the developed module faithfully represent the actual probe head error values, which means that the module can be successfully implemented in the digital metrological twin model of a five-axis CMM.

CMM, digital twin, accuracy, five-axis, uncertainty

1. Introduction

In recent years, a rapid development of solutions in the field of artificial intelligence has been observed, resulting in numerous applications also within the domain of geometric metrology [1]. Potential areas of application of this technology include, among others, the identification of errors in coordinate measuring machines [2], support of surface roughness evaluation processes [3], errors correction of optical measuring systems [4] and measurement uncertainty estimation [5]. In the latter area, methods based on various forms of machine learning align with the ongoing trend toward the development of simulation-based approaches for assessing measurement accuracy.

These methods, offering a number of undeniable advantages such as high computational efficiency and usability by operators without extensive expertise in measurement uncertainty, constitute a highly desirable alternative to classical approaches, such as the calibrated-workpiece method [6] or the guidelines described in the GUM [7]. Although the well-known methods of uncertainty estimation are supported by numerous application examples and well-defined computational frameworks, they still pose a significant challenge in practice, as evidenced by the ambiguity of results obtained by different institutions [8].

This article presents a description and the results of an experimental study focused on the use of artificial neural networks for modelling the errors of a measurement probe employed in a five-axis coordinate measuring system. The importance of this system component requires no further justification [9], while in five-axis systems the probe plays a critical role by fundamentally influencing the measurement process and enabling improvements in both accuracy and repeatability [10]. The subsequent sections describe the development of the AI-based model for probe errors and its comparison with experimental results as well as with an existing error model for this type of probe.

2. Methodology and Experiments

The described investigations were carried out on a five-axis coordinate measuring system consisting of a Zeiss WMM 850S coordinate measuring machine and a Renishaw PH20 probe head mounted on its quill, operating in conjunction with a TP20 SF touch-trigger probe (Fig.1). The system working volume is 800 × 1000 × 600 mm, and its accuracy can be described as (1):

$$E_{E0,MPE} = 2{,}5 + 2{,}5 * L/1000 \qquad (1)$$

where: L is measured length given in mm

Figure 1. Five-axis coordinate system utilized during experiments consisting of Zeiss WMM 850S with installed probing system Renishaw PH20.

Accuracy of probing system can be characterized with a PForm.Sph.1x25:SS:Tact value of 0.0021 mm. The PH20 probe head constitutes a key component of the five-axis system, as it enables measurements to be performed using the rotational motions of the probe head rather than, as in conventional CMMs with a fixed declared probe orientation, relying on the linear movements of the measuring machine itself.

The probe head features two rotary axes whose theoretical point of intersection lies on the quill axis responsible for motion along the vertical direction. The vertical rotation angle is denoted by the letter B and can vary within the range from −180° to 180°, while the horizontal rotation angle is denoted by A and can vary from −100° to 100°. The probe stylus is aligned parallel to the quill axis when the angular positions are set to A = 0° and B = 0°.

The data required for the model (treated as input data) were obtained through repeated measurements of a reference ring with a diameter of 20 mm and a small form deviation (approximately 0.2 µm), performed in various orientations relative to the working range of the probing system. Each ring orientation was defined by the A and B angle values, which represent the angular positions of the probing system when it is oriented parallel to the main axis of the reference ring. Measurements were carried out with the B angle varying in increments of 20° from −160° to 180°, and the A angle varying in increments of 15° from 0° to 90°. For each ring orientation, the ring was measured at 64 evenly distributed points located at the mid-height of the ring (Fig. 2).

Figure 2. Five-axis coordinate system utilized during experiments consisting of Zeiss WMM 850S with installed probing system Renishaw PH20.

A local coordinate system was established using the inner cylindrical surface of the ring gauge (as the main spatial axis), the ring plane (to define the datum origin), and measurements of one side of the block to which the ring was attached (to define the second direction of the coordinate system). During the circle measurements, only the movements of the probing system were employed. The radial error at each measured point was determined relative to a least-squares fitted circle. Such errors due to small size of reference ring (diameter of 20 mm) and its small form deviation (about 0,2 µm) can be treated as a representation of probing system errors [11]. For each orientation, the measurements were repeated ten times.

The results obtained for approximately 120 orientations were used as input data for the AI model, comprising about 76,000 measured points and corresponding deviations. Some of the orientations measured during the experiment were deliberately excluded from the input dataset to allow their subsequent use for verification of the model's performance.

The AI model architecture consists of three main dense blocks. The first two hidden layers each had 256 neurons, and the third layer had 128 neurons. Layer Normalization (LN) and GELU nonlinearity were applied after each of the first two layers, followed by a 0.10 dropout to reduce overfitting and improve generalization for unseen pairs (A, B). After the third layer, normalization and GELU activation without dropout were applied to preserve the model's ability to accurately estimate small values. The output layer was linear and returned a vector of 1+2K Fourier coefficients; for the example configuration K=8, this means 17 output parameters. Additionally, L2 regularization (of the order of 10^{-4}) was applied to the dense layers, acting as a mild constraint on model complexity, especially important when the number of unique configurations (A, B) is small. The coefficients predicted by the network were transformed to $\hat{d}(n)$ values at each training iteration by matrix multiplication with a Fourier basis matrix corresponding to a 64 number of measured points n. The d'(n) waveform was then compared to the reference d(n), minimizing the weighted Huber loss. The mean absolute error (MAE) and RMSE, also calculated at the full curve level in µm, were used as diagnostic metrics.

Optimization was performed using the AdamW method, an Adam variant with explicit weight decay, with an initial training step of 10^{-3} and a weight decay of 10^{-4}. The training process was supported by a ReduceLROnPlateau learning step reduction schedule that monitored the MAE validation metric of the curve, with the minimum learning step limited to 10^{-6}, and a patient Early Stopping mechanism, which allowed for a stable approach to the optimum without the risk of quality degradation in the validation set. A key element of the validation protocol was the division of the data into training, validation, and test sets, implemented at the group level (A,B), so that the probe head configurations in the test set were not visible during training.

After the AI model was created, it was used in the next step to predict error values at individual measurement points for the selected orientations that had been measured but were not included in the model input dataset. The model predictions were compared with the results obtained from direct measurements and with those simulated using an error model based on trilinear interpolation combined with the Monte Carlo method, as described in [12]. For each point, the simulation error ε_s was determined according to the following equation (2):

$$\varepsilon_s = \delta_{AI} - \delta_m \tag{2}$$

where: δ_{AI} – deviation given by AI model; : δ_m – deviation obtained through measuremnts

3. Results and discussion

In the following figures, the results obtained from measurements of the ring, as well as those given by the AI model and the trilinear interpolation model, are presented. The verification was performed at the following positions: A 15, B -20 (Fig. 3), A 75, B 40 (Fig. 4), and A 45, B -20 (Fig. 5). Additionally, measurements were conducted at an extra position located between the orientations considered in the model: A 43, B 91 (Fig. 6).

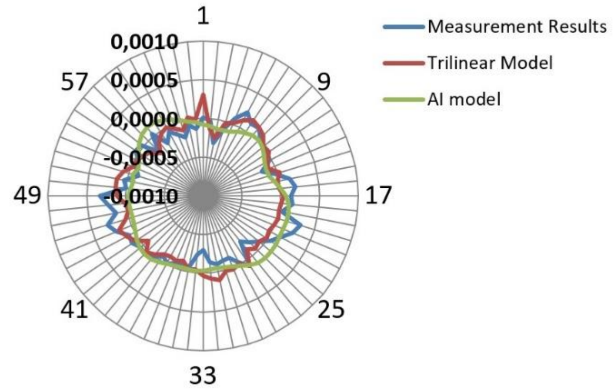

Figure 3. Ring orientation **A 15 B -20**. Results of verification of developed AI model and its comparision with probing system errors model based on usage of trilinear interpolation and Monte Carlo method. The error values are represented along the radial axis expressed in mm. The values indicated along the circumference represent the measurement points numbers.

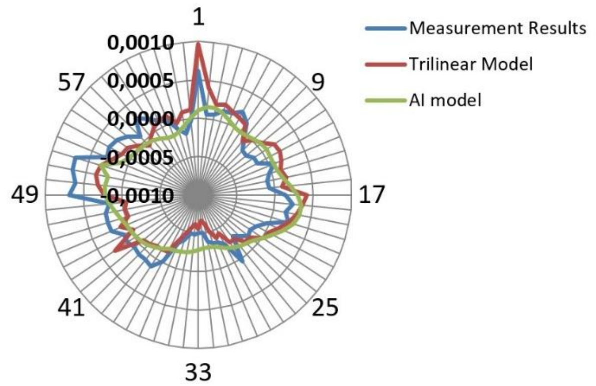

Figure 4. Ring orientation **A 75 B 40**. Results of verification of developed AI model and its comparision with probing system errors model based on usage of trilinear interpolation and Monte Carlo method. The error values are represented along the radial axis expressed in mm. The values indicated along the circumference represent the measurement points numbers.

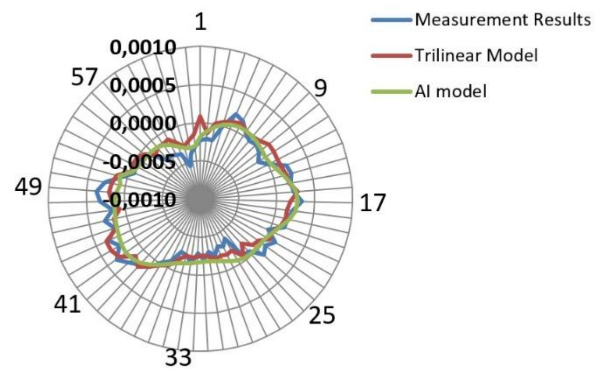

Figure 5. Ring orientation **A 45 B -20**. Results of verification of developed AI model and its comparision with probing system errors model based on usage of trilinear interpolation and Monte Carlo method. The error values are represented along the radial axis expressed in mm. The values indicated along the circumference represent the measurement points numbers.

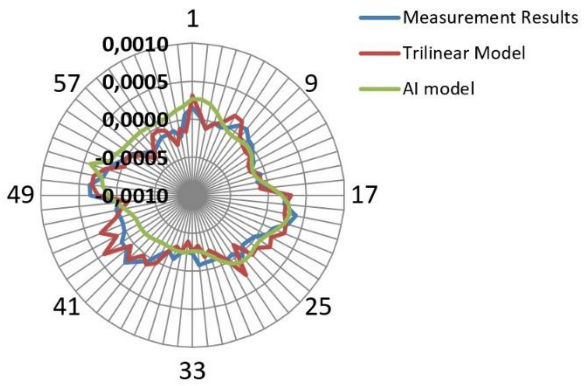

Figure 6. Ring orientation **A 43 B90**. Results of verification of developed AI model and its comparision with probing system errors model based on usage of trilinear interpolation and Monte Carlo method. The error values are represented along the radial axis expressed in mm. The values indicated along the circumference represent the measurement points numbers.

A characteristic feature of the PH20 probe head is the change in the error distribution obtained when measuring the same ring using different orientations [12]. The AI model was able to reproduce this variation. When analyzing the presented plots, it should be noted that both error models considered in the experiment yielded overall error characteristics that are similar in shape to those obtained from the measurements. However, it is evident that the AI model performed less effectively in reproducing sudden irregularities in the error characteristics, tending instead to smooth the probe head error values.

Below, Tables 1–3 present a ranges of probe errors obtained from measurements and modelled using considered models, the maximum absolute probe head error and the mean absolute simulation error.

Table 1 Range calculated from probe errors obtained for different orientations of reference ring from measurements and via simulation using AI model and trilinear interpolation model. Range values given in µm.

Ring orientation	Range / µm		
	Measurement	AI model	Trilinear model
A 15 B -20	0,60	0,70	0,60
A 75 B 40	1,20	0,80	0,80
A 45 B -20	0,90	0,60	0,50
A 43 B 90	0,60	0,80	0,60

Table 2 . Maximum absolute value of of probe error obtained for different orientations of reference ring from measurements and via simulation using AI model and trilinear interpolation model. Error values given in µm.

Ring orientation	Maximum absolute probe error / µm		
	Measurement	AI model	Trilinear model
A 15 B -20	0,30	0,40	0,30
A 75 B 40	0,70	0,50	0,97
A 45 B -20	0,60	0,33	0,31
A 43 B 90	0,40	0,50	0,40

Table 3 Mean absolute simulation error in relation to experimentaly obtained data for AI model and trilinear interpolation model. Error values given in µm.

Ring orientation	Mean absolute simulation error / µm	
	AI model	Trilinear model
A 15 B -20	0,12	0,11
A 75 B 40	0,18	0,17
A 45 B -20	0,11	0,13
A 43 B 90	0,14	0,10

An analysis of the obtained error results indicates that both models generated very similar values. It is difficult to unequivocally determine which model is closer to the reference values obtained from the measurements, as in nearly every considered case, for two of the ring orientations the AI model produced results that were more accurate or more consistent with the measured values, while for the remaining two orientations better agreement was achieved by the model based on trilinear interpolation combined with the Monte Carlo method.

What deserves particular attention and emphasis is the fact that the observed discrepancies with respect to the measurement-derived errors are on the order of a few tenths of a micrometer. Moreover, for none of the considered ring orientations does the mean absolute simulation error exceed 0.2 µm. Taking into account that the manufacturer of the TP20 probe, which is mounted on the PH20 probe head, specifies a pre-travel variation of ±0.8 µm for the standard trigger force version and a unidirectional repeatability of ±0.35 µm, as well as that PForm.Sph.1x25:SS:Tact of the utilized five-axis system is about of 2 µm the observed results should be regarded as highly satisfactory.

Considering only the results presented in Tables 1–3, it can be concluded that the AI-based model could perform sufficiently well as a component of a digital twin for measurement uncertainty estimation in the context of probe head error modeling in a five-axis coordinate measuring system.

At the same time, it is important to acknowledge a limitation of the proposed solution. As noted in the Materials & Methods section, the training of the model required probe head error information obtained at nearly 75,000 measurement points. This is a large dataset, implying the need for extensive and time-consuming experimental campaigns. By comparison, the model based on trilinear interpolation and the Monte Carlo method relies on error information observed at approximately 15,000 points. Although this still represents a substantial amount of measurement data, it nonetheless requires roughly five times less experimental effort

4. Conclusions

The presented AI-based model for generating probe head errors in five-axis coordinate measuring systems achieved satisfactory agreement with experimentally obtained data. The error characteristics produced by the AI model are slightly smoothed compared to the measurement data, which may suggest that, in its current form, the model would be difficult to apply directly for probe head error compensation. At the same time, as demonstrated by the verification experiments conducted for different orientations of the reference ring, the model was able to capture changes in the error distribution across different regions of the probe head working volume so it seems that it could be useful in estimation of measurement uncertainty.

The observed simulation errors, determined with respect to experimentally acquired values, were significantly lower than the probe head repeatability declared by the manufacturer. However, the most significant limitation of the current model is the requirement for a large amount of input data, which raises concerns regarding its practical applicability. When comparing the AI-based approach with another model reported in the literature [12], no clear advantages of the AI model can be identified. Considering a substantially larger number of preliminary measurements required for the AI model than for the one based on trilinear interpolation combined with the Monte Carlo method, the use of AI in this specific case does not appear to be the most effective available option. This finding may serve as an argument against the prevailing tendency to apply AI indiscriminately to all possible applications and problem domains.

References

[1] Wieczorowski M, Kucharski D, Sniatala P, Pawlus P, Krolczyk G and Gapinski B 2023 *Meas.* **217** 113051

[2] Chen G, Mehdi-Souzani C, Anwer N 2026 *Adv. Eng. Inform.* **70** 104142

[3] Yang H, Zheng H and Zhang T 2024 *Tribol. Int.* **199** 109935

[4] Harmatys W, Gąska A, Gąska P and Gruza M 2026 *Meas.* **260** 119863

[5] Samadi H, Ahsan M and Raman S 2025 *Next Research* **2** 100299

[6] ISO 15530-3:2011 GPS CMM Use of calibrated workpieces or measurement standards

[7] JCGM 100, Evaluation of measurement data. Guide to the expression of uncertainty in measurement, 2008

[8] Hansen H N and De Chiffre L 1999 *Prec. Eng*. **23** 3 185-195

[9] Weckenmann A, Estler T, Peggs G and McMurtry 2004 CIRP Ann. Manuf. Technol. 53 2 657-684

[10] Gruza M, Gąska A, Gąska P, Harmatys W and Sładek J 2016 Mechanik 11 1708-1709

[11] Sładek J 2016 Coordinate Metrology Accuracy of Systems and Measurements Springer: Berlin, Germany

[12] Gąska A, Gąska P and Gruza M 2016 Appl. Sci.6 144